Cellular Motions and Thermal Fluctuations: The Brownian Ratchet

Charles S. Peskin,* Garrett M. Odell,[‡] and George F. Oster[§]

*Courant Institute of Mathematical Sciences, New York, New York 10012; [‡]Department of Zoology, University of Washington, Seattle, Washington 98195; [§]Departments of Molecular and Cellular Biology, and Entomology, University of California, Berkeley, California 94720 USA

ABSTRACT   We present here a model for how chemical reactions generate protrusive forces by rectifying Brownian motion. This sort of energy transduction drives a number of intracellular processes, including filopodial protrusion, propulsion of the bacterium *Listeria*, and protein translocation.

INTRODUCTION

Many types of cellular protrusions, including filopodia, lamellipodia, and acrosomal extension do not appear to involve molecular motors. These processes transduce chemical bond energy into directed motion, but they do not operate in a mechanochemical cycle and need not depend directly upon nucleotide hydrolysis. In this paper we describe several such processes and present simple formulas for the velocity and force they generate. We shall call these machines "Brownian ratchets" (BR) because rectified Brownian motion is fundamental to their operation.[1] The systems we address here are different from those usually considered protein motors (e.g., myosin, dynein, kinesin), but such motors may be Brownian ratchets as well (1–4).

Consider a particle diffusing in one dimension with diffusion coefficient D. The mean time it takes a particle to diffuse from the origin, $x = 0$, to the point $x = \delta$ is: $T = \delta^2/2D$. Now, suppose that a domain extending from $x = 0$ to $x = L$ is subdivided into $N = L/\delta$ subintervals, and that each boundary, $x = n \times \delta$, $n = 1, 2, \ldots, N$ is a "ratchet": the particle can pass freely through a boundary from the left, but having once passed it cannot go back (i.e., the boundary is absorbing from the left, but reflecting from the right). The physical mechanism of the ratchet depends on the situation; for example, the particle may be prevented from reversing its motion by a polymerizing fiber to its left. The time to diffuse a length δ is $T_\delta = \delta^2/2D$. Then the time to diffuse a distance $L = N \times \delta$ is simply $N \times T_\delta$: $T = N \times T_\delta = N (\delta^2/2D) = L(\delta/2D)$. The average velocity of the particle is $v \equiv L/T$, and so the average speed of a particle that is "ratcheted" at intervals δ is

$$v = \frac{2D}{\delta}.$$

This is the speed of a perfect BR. Note that as the ratchet interval, δ, decreases, the ratchet velocity increases. This is because the frequency of smaller Brownian steps grows more rapidly than the step size shrinks (when δ is of the order of a mean free path, then this formula obviously breaks down).

Several ingredients must be added to this simple expression to make it useful in real situations. First, the ratchet cannot be perfect: a particle crossing a ratchet boundary may occasionally cross back. Second, in order to perform work, the ratchet must operate against a force resisting the motion. To characterize the mechanics of the BR we shall derive load-velocity relationships similar to the Hill curve that summarizes the mechanics of muscle contraction.

HOW DOES POLYMERIZATION PUSH?

In discussions of cell motility it is frequently asserted that the polymerization of actin or of microtubules can exert a mechanical force. This assertion is usually buttressed by thermodynamic arguments that show that the free energy drop accompanying polymerization is adequate to account for the mechanical force required (5). Aside from the fact that thermodynamics applies only to equilibrium situations, such arguments provide no mechanistic explanation of how the free energy of polymerization is actually transduced into directed mechanical force. Here we present a mechanical picture of how polymerizing filaments can exert mechanical forces.

Filopodia

Janmey was able to load actin monomers into liposomes and trigger their polymerization (6). He observed that the polymerizing fibers extruded long spikes resembling filopodia from the otherwise spherical liposomes. A similar phenomenon was described by Miyamoto and Hotani (7) using tubulin. This demonstrates that polymerization can exert an axial force capable of overcoming the bending energy of a lipid bilayer without the aid of molecular motors such as myosin. Using a bilayer bending modulus of $B = 2 \times 10^{-12}$ dyne-cm (8, 9), the energy required to elongate a lipid cylinder of radius 50 nm from zero length to 5 μm long is

[1] To avoid confusion we reserve the term "thermal ratchet" to denote engines that employ a temperature gradient. Brownian ratchets operate isothermally, with chemical energy replacing thermal gradients as the energy source.

$\sim 2 \times 10^4$ $k_B T$.[2] Since we are dealing with thermal motions, henceforth we will express all energetic quantities in terms of $k_B T \sim 4.1 \times 10^{-14}$ dyne-cm, where k_B is Boltzmann's constant and T is the absolute temperature. The free energy change accompanying actin polymerization is $\Delta G \sim -14$ $k_B T$/monomer (10). So, polymerization can provide sufficient free energy to drive membrane deformation (5, 11). The BR model provides an explanation for how this free energy is transduced into an axial force.

Consider the ratchet shown in Fig. 1. An actin rod polymerizes against a barrier (e.g., a membrane) whose mobility we characterize by its diffusion coefficient, D. We model a polymerizing actin filament as a linear array of monomers; here, the ratchet mechanism is the intercalation of monomers between the barrier and the polymer tip. Denote the gap width between the tip of the rod and the barrier by x, and the size of a monomer is indicated by δ. When a sufficiently large fluctuation occurs the gap opens wide enough to allow a monomer to polymerize onto the end of the rod. The polymerization rate is given by $R = k_{on}(x) \times M - \beta$, where M is the local monomer concentration and $k_{on}(x) \times M$, reflects the *conditional* probability of adding a monomer when the gap width is x. We set $k_{on}(x) \times M = \alpha$ when $x \geq \delta$, and $k_{on}(x) \times M = 0$ when $x < \delta$. If no barrier were present, actin could polymerize at a maximum velocity of $\delta \times R \sim 0.75$ μm/s at 25 μM concentration of actin monomers (12). Cellular filopodia protrude at velocities about 0.16 μm/s (13), well below the maximum polymerization rate. In Appendix A we show that the polymerization BR obeys the equation

$$\frac{\partial c}{\partial t} = D \frac{\partial^2 c}{\partial x^2} + \left(\frac{fD}{k_B T}\right) \frac{\partial c}{\partial x} + \alpha[c(x + \delta, t) - H(x - \delta)c(x,t)]$$

$$+ \beta[H(x - \delta)c(x - \delta, t) - c(x,t)] \qquad (1)$$

where $c(x,t)$ is the density of systems in an ensemble at position x and time t. Here D is the diffusion coefficient of the particle, $-f$ is the load force (i.e., to the left, opposing the motion), $H(x - \delta)$ is the Heaviside step function (= 0 for $x < \delta$, and = 1 for $x > \delta$). The boundary conditions are that $x = 0$ is reflecting and that $c(x,t)$ is continuous at $x = \delta$. The

[2] If we model a filopod as a cylinder with a hemispherical cap, then we can compute how much energy it takes to form such a structure from a planar bilayer. Using B $\sim 50k_B T$, the energy required to bend a membrane into a hemispherical cap is $W = 4\pi B \sim 600\ k_B T$. To create a membrane cylinder of radius 50 nm and $L = 1$ μm costs $\sim 3000\ k_B T/\mu$m. To elongate by 1 ratchet distance, $\delta = 2.5$ nm, against a membrane tension of about $\sigma = 0.035$ dyne/cm (equivalent to a load force of ~ 11 pN) costs $\sim 6.6\ k_B T$, so that a protrusion of 5 μm requires $\sim 1.3 \times 10^4\ k_B T$ of work. Thus the total work to create a filopod 5 μm long and 50-nm radius $= 2 \times 10^4\ k_B T$. The binding energy of an actin monomer is $\sim -13.6\ k_B T$/monomer, making the process 8/13.6 $\sim$60% efficient. Each monomer, before attaching to the filament, binds one ATP which is hydrolyzed sometime after the monomer attaches. Each hydrolysis yields about $\Delta G \sim$ 15–20 $k_B T$/mol $\sim$62 pN-nm/ATP; if we were to add this to the ATP; contribution we would have a total free energy drop of $\Delta G \sim -30\ k_B T$/monomer. However, since ATP is hydrolyzed after polymerization its contribution to force generation is not important. The viscous work against the fluid medium is inconsequential compared to the bending energy, so we can neglect it in this estimate.
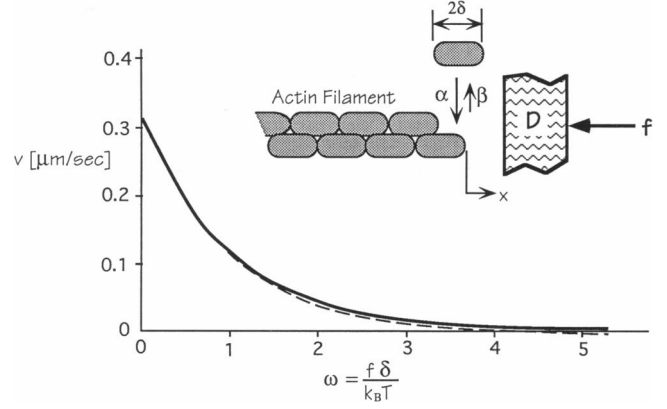

FIGURE 1 The polymerization ratchet. An actin filament polymerizes against a barrier with diffusion constant D upon which a load, f, acts. Because the filaments are arranged in a paired helix, we model the ratchet distance, δ, as half the size of a monomer. The the graphs shows the speed of the polymerization ratchet, v (μm/s), driven by a single actin filament, as a function of dimensionless load force, $\omega = f \times \delta/k$B. The solid line is based on Eq. 2, the formula for the ratchet speed when depolymerization is negligible ($\beta \to 0$). The curve was plotted by using μ as a parameter, i.e., $\mu \to [\omega(\mu), v(\mu)]$. The dashed line is based on Eq. 3, valid when polymerization is much slower than diffusion, $\alpha\ \delta^2/D \ll 1$ and $\beta\ \delta^2/D \ll 1$. The rate constants were taken from Pollard (12) for actin polymerization: $\alpha = k_{on} \times M = 11.3$ [1/s $\times$ μM] $\times$ 10[μM], $\beta = 1.6$ [1/s], $\delta =$ (monomer size)/2 $\sim 2.7 \times 10^{-7}$ cm, since actin is a double helix). We used a load diffusivity of $D = 1 \times 10^{-9}$ cm^2/s, corresponding to a disk of diameter ~ 2.5 μm. Filopodial velocities are below 0.16 μm/s (13), which is about 20% of the maximum polymerization velocity, $\delta \times (\alpha - \beta) = \delta \times (k_{on} \times M - k_{off}) \sim$ 0.76 μm/s (12, 27). From Eq. 4, the stall force for a single actin fiber is $f_0 \sim 7.8$ pN. A filopod composed of 20 filaments presumably could exert 20 times this force.

steady state solution to Eq. 1 gives the force-velocity relation if we define the ratchet velocity by

$$v = \delta\ \frac{\alpha \int_\delta^\infty c(x)\ dx - \beta \int_0^\infty c(x)\ dx}{\int_0^\infty c(x)\ dx)}$$

(i.e., we weight the polymerization velocity by the probability of a δ-sized gap). When depolymerization can be neglected, i.e., $\beta \ll \alpha$, which is the case for actin polymerization, we obtain the load-velocity relationship:

$$v = \frac{2D}{\delta}\left[\frac{(\mu - \omega)\ (\omega^2/2)}{\omega^2 + (e^\infty - \omega - 1)\mu}\right] \qquad (2)$$

where ω is the dimensionless work done against the load in adding one monomer: $\omega = f \times \delta/k_B T$, and $\mu(\omega, \delta, \alpha, D) > \omega$ is given by solving a transcendental equation, $\mu - \omega = (\alpha\ \delta^2/D)\ [1 - \exp(-\mu)])/\mu$. Fig. 1 shows a plot of $v(\omega)$. If the polymerization and depolymerization velocities are much slower than the ideal ratchet velocity, i.e., $\alpha \times \delta$, $\beta \times \delta \ll 2D/\delta$, then the ratchet equation can be solved explicitly for $\beta \neq 0$. The result is a startlingly simple formula:

$$v = \delta[\alpha e^{-\omega} - \beta] \qquad (3)$$

That is, the polymerization rate, $\alpha = k_{on} \times M$, is weighted by the probability of the load allowing a monomer-sized gap, δ. Note that in this limit the ratchet velocity does not depend

on the diffusion coefficient of the load. Membrane tensions fall in the range 0.035–0.039 dyne/cm, which amount to a load force of about 25 pN. A filopod of 20 filaments could produce a thrust 20 times as strong as a single filament, or about 200 pN. The force required to stall the ratchet is found by setting $v = 0$ in Eq. 3, which yields the familiar thermodynamic relationship $\beta/\alpha = \exp(-f \times \delta/k_B T)$, or

$$f_0 = -\frac{k_B T}{\delta} \ln\left(\frac{\beta}{\alpha}\right). \tag{4}$$

This formula for the stall force is exact; it remains valid for all parameter values, even those that violate the assumptions used in deriving Eq. 3.

Two observations support the BR model for filopodial growth. First, the velocity of extension is almost constant (13), unlike the acrosomal extension of *Thyone* sperm, in which length grows as the square root of time (14–19). The BR mechanism produces a constant velocity provided that the polymerization affinity is constant. Eventually, the filopod may grow long enough so that the diffusion of actin monomers to the tip is limiting, in which case the velocity will decrease. Second, experiments by Bray et al. (20) demonstrated that filopodial extension velocities actually increased somewhat with external osmolarity. This is consistent with the BR mechanism, since pulling water out of the cell will concentrate the actin monomers, thus increasing the affinity for a time, and hence the ratchet velocity. This contrasts with acrosomal protrusion of *Thyone* wherein increasing the external osmolarity decreases protrusion velocities (17–19). However, once a filopod grows long enough so that diffusion limits the concentration of actin monomers at the tip, the protrusion velocity will fall to zero quite quickly.

The BR formula omits an important feature: proteins are flexible, elastic structures, whose internal fluctuations significantly affect their motions. In the ratchet formula (2) the rod is assumed to be stiff and the gap width depends solely on the diffusion of the barrier. However, since the actin monomers are themselves flexible, Brownian motion will induce thermal "breathing" modes which will contribute to the gap width. There is no simple way to include this into the model; however, we can use numerical simulations to investigate elastic effects in particular situations. We have performed a molecular dynamics simulation of this situation using the parameters for actin; the details of this computation will be published elsewhere. We find that for rod lengths of more than 50–100 monomers the fluctuations within the rod can compress the rod enough to permit polymerization even if the barrier is too large to diffuse appreciably. In this situation the elastic compression energy generated by thermal motions is the proximal origin of the force.

Listeria propulsion

The bacterium *Listeria monocytogenes* moves through the cytoplasm of its host cell with velocities typically between 0.02 and 0.2 μm/s (21), but as fast as 1.5 μm/s in some cells (22, 23). As it moves, it trails a long tail of polymerized actin

consisting of many short fibers cross-linked into a meshwork; the fibers are oriented predominantly with the barbed end in the direction of motion (22, 23). Using fluorescent photoactivation Theriot et al. (21) were able to visualize the tail as the bacterium moved. They found that the tail remained stationary, and that actin inserted into the tail meshwork adjacent to the bacterial body. Taken together, these observations suggest that actin polymerization may drive bacterial movement (21, 24).

We propose that *Listeria is* driven by the BR mechanism: the polymerizing tail rectifies the random thermal motions of the bacterium, preventing it from diffusing backwards, but permitting forward diffusion. In this view the tail doesn't actually push the bacterium: propulsion is simply Brownian diffusion rendered unidirectional by the polymerization of the actin tail. This could work in several ways. For example, assume the bacterium diffuses as a Stokes particle of size ~1 μm (25), and the polymerization rate constants are the same as we used in the filopod calculation (12, 26). If the elastic resistance of the cell's dense actin gel is the major impediment to the bacterium's motion, it may be reasonable to ascribe the load force to this elastic resistance. Then the ratchet formula predicts velocities in the correct range working against a load of a few piconewtons. The velocity depends on the effective concentration of actin monomers near the bacterium. The in vitro concentration is unknown, but is likely to be much higher than at the tip of a filopod. Using an effective local concentration of 50 μM (27), the stall force for a single actin fiber is $f_0 \sim 9$ pN, about six times the force generated by a myosin crossbridge. Since the tail consists of many fibers, whose orientations are not collinear, we cannot directly compute the thrust of the tail without knowledge of the fiber number and orientation distributions. All we can say is that the computed load-velocity curve shows that one fiber would be sufficient to drive a 1-μm bacterium at 1.5 μm/s against a load of 1 pN. This calculation assumes that the Brownian motion of the bacterium is the same as it would be in fluid cytoplasm. However, the average mesh size of the cortical actin gel is in the neighborhood of 0.1 μm, about 1/10th the size of the bacterium, and so the gel may constrain the bacterium's Brownian motion substantially. This can produce an apparent cytoplasmic viscosity of more than 100 poise, which would reduce the ratchet velocity considerably. However, molecular dynamics simulations demonstrate that the elastic breathing modes of the actin tail fibers discussed above can still drive the motion of the bacterium at the observed velocities. We will report on these simulations elsewhere.

According to the BR mechanism the speed of the BR depends on the polymerization rate of actin, although it is not *driven* directly by the polymerization. The faster the bacterium can recruit actin from the cytoplasmic pool the faster the bacterium moves and the longer the tail grows. Theriot and Mitchison (21) found that the velocity was proportional to tail length. In Appendix C we show that this linear relationship between velocity and tail length holds quite generally, regardless of the mechanism of force generation. Using

a laser trap it should be possible to measure the stall force as a function of monomer concentration, which Eq. 4 predicts should vary as $f_o \sim \ln(M)$. In vivo values of diffusion coefficients and monomer concentrations may be quite different from those in vitro; and so our computed load-velocity curve is probably not too accurate. In order to characterize the *Listeria* BR motor, it is necessary to design experiments to measure accurately the diffusion coefficient of a "dead" bacterium along with the in situ polymerization rates and the fiber orientations.

A possible analog of the *Listeria* system was reported recently by Forscher et al. (28): polycationic beads dropped onto the surface of certain cells commenced to move in the plane of the membrane at speeds of about 0.16 μm/s. Closer inspection revealed a tail of polymerized actin streaming behind the moving bead. This resembles the tail of *Listeria*, and it is tempting to assert that this too is a manifestation of the Brownian ratchet mechanism.

PROTEIN TRANSLOCATION

Recently, we proposed that post-translational translocation of a protein across a membrane may be driven by a BR (29).

We addressed the process that begins after the proximal tip of the protein is threaded through the translocation pore (30). Brownian motion causes the protein to fluctuate back and forth through the pore, but with no net displacement in either direction (analogous to a reptating polymer (31)). If a chemical modification of the protein occurs on the distal side of the membrane which inhibits the chain from reptating back through the pore, the chain will be ratcheted. The model assumes that the protein is maintained in an unfolded conformation so that it is free to fluctuate back and forth through the translocation pore. This is accomplished in the cell by the ribosomal tunnel in the case of cotranslational translocation, and by chaperonins in the case of post-translational translocation. There are several known chemical asymmetries that can bias the Brownian walk of a chain (cf. Fig. 2) (29, 32–34). As a polypeptide emerges from the translocation apparatus the chain is subjected to glycosylation, formation of disulfide bonds, cleavage of the signal sequence (which affects folding of the chain, and binding of chaperonins). Any, or all, of these can induce the asymmetry in the system required for the BR. This multiplicity of ratchet mechanisms may explain why different laboratories have attributed the translocation motor
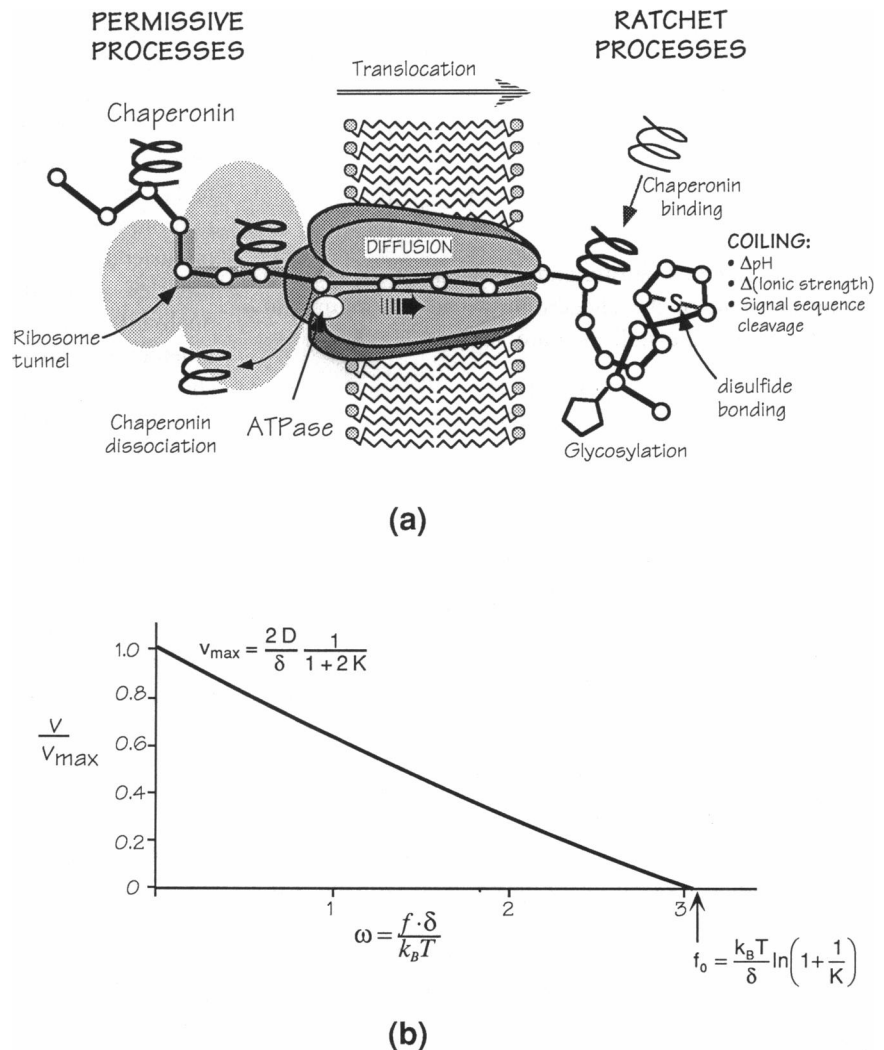

FIGURE 2 (*a*) Diffusion of a protein through the translocation pore depends on permissive events on the cytoplasmic side of the membrane and ratcheting events on the lumenal side. In order to enter the pore the protein must be maintained in an extended state. This is accomplished for posttranslational translocation by binding of chaperonins, and for cotranslational translocation by the ribosomal tunnel (the drawing is not intended to imply the two act concurrently). On the lumenal side the reptation of the protein through the pore can be ratcheted by several processes: disulfide bond formation, glycosylation, and conditions that enhance chain coiling, including differences in pH, ionic strength across the membrane, and cleavage of the signal sequence. (*b*) The dimensionless load-velocity curve for the translocation ratchet. $\omega = f \times \delta/k_B$ is the dimensionless load. The maximum velocity and stall load are given by Eqs. 6 and 7.

$$v_{max} = \frac{2D}{\delta} \frac{1}{1+2K}$$

$$\omega = \frac{f \cdot \delta}{k_B T}$$

$$f_0 = \frac{k_B T}{\delta} \ln\left(1 + \frac{1}{K}\right)$$

(a)

(b)

to different constituents of the translocation machinery, and why almost any protein can be translocated if given the proper signal sequence.

This ratchet is somewhat different from the polymerization BR considered above since there are many ratcheting sites rather than one. In Appendix B we derive a force-velocity relationship for the translocation ratchet in the case where the ratchet mechanism is the binding of chaperonins on the luminal side of the translocation pore. Since the motion of each segment is equivalent we consider an ensemble of points diffusing on a circle of circumference equal to the length of a ratchet segment of the polymer, δ. As before, each point is subject to a force $-f$ which imparts a drift velocity $-f \times D/k_B T$. Points are in rapid equilibrium between two states: $S_o \rightleftarrows S_1$, with rate constants k_{on} and k_{off}. Points in state S_o pass freely through the origin in both directions, but points in state S_1 are ratcheted: they cannot cross back across the origin. Let p be the probability of finding a point in state S_1: $p = k_{on}/(k_{on} + k_{off})$. Then we can write the net flux of points as $\phi(x, t) = -(Df/kT)c - D(\partial c/\partial x)$, where $c(x, t)$ is the density of points at position x and time t. $\phi(x)$ satisfies the steady state conservation equation $(\partial \phi/\partial x) = 0$, with boundary conditions $\phi(0) = \phi(\delta)$, and $c(\delta) = (1-p) \times c(0)$. (The latter boundary condition is not self-evident; it is derived in Appendix B.) We solve for $c(x)$ and define the average velocity as $v = \delta\phi/N$, where $N = \int_0^\infty c(x, t)\, dx$ is the total number of points in the ensemble. The result is:

$$v = \frac{2D}{\delta} \left[\frac{\frac{1}{2}\omega^2}{\left(\frac{(e^\omega - 1)}{1 - K(e^\omega - 1)}\right) - \omega} \right] \quad (5)$$

where ω is defined as before, and the parameter is the dissociation constant of the chaperonins. The maximum (no load) velocity and the stall load are:

$$v_{max} = \frac{2D}{\delta}\frac{1}{1 + 2K}, \quad (6)$$

$$f_0 = \frac{k_B T}{\delta} \ln\left(1 + \frac{1}{K}\right). \quad (7)$$

Note that even when $K = 1$, translocation still proceeds at a finite rate, whereas the polymerization ratchet stalls even in the no-load condition when $\alpha = \beta$. A typical force-velocity curve computed from Eq. 5 is plotted in Fig. 2. Equation 5 has two important limitations. First, it assumes that the rates k_{on} and k_{off} are very fast, and second, that the ratchet is inelastic. The effect of elasticity cannot be handled analytically; however, numerical studies show that an elastic chain translocates faster than a rigid chain (29). This is because local fluctuations can carry a subunit through the pore to be ratcheted without translocating the entire chain. Note that Eq. 6 implies that the average translocation time for a free chain of length L is $T = L/v \propto L \times \delta$; for a chain of length $L = n \times \delta$, $T \propto \delta^2$. Numerical simulations show that this quadratic dependence on ratchet distance is obeyed for elastic chains as well (29).

Since there is no obvious load force resisting translocation, we can use Eq. 6 to put some quantitative bounds on the translocation time of a protein. For example, the slowest time corresponds to the situation where one end is just threaded through the translocation pore and translocation is completed when the other end passes through the translation pore. Taking $\delta \sim 100$ nm as the length of an unfolded protein, and $D \sim 10^{-8}$ cm^2/s as the longitudinal diffusion coefficient, the translocation time is ~ 5 ms; but if the chain is ratcheted every 5 nm, the transit time is 0.25 ms—faster by a factor of 20. This estimate of τ is probably too short, since the one-dimensional formula (6) cannot take into account the effects of chain coiling; for this a full three-dimensional calculation must be carried out. Also, Eq. 5 neglects the effect of chain elasticity, which significantly adds to the translocation velocity. Thus, both our numerical and analytical calculations demonstrate that the BR mechanism is more than sufficient to account for the observed rates of translocation. Recent experiments by Ooi and Weiss (35) have confirmed the predictions of the BR model. They found that proteins targeted to liposomes could translocate bidirectionally through the translocation pore. However, if the lumen contained the chaperonin BiP, or if lumenal glycosylation was enabled, proteins translocated unidirectionally.

There are several other phenomena that are possibly driven by rectified diffusion. For example, the polymerization of sickle hemoglobin into the rods that deform the erythrocyte membrane appear similar to filopod protrusion (36), and probably derive their thrust from the same mechanism. Finally, in vitro model systems show that depolymerizing microtubules can drive kinetochore movements toward the minus end at velocities of ~ 0.5 μm/s and exert forces on the order of $\sim 10^{-5}$ dyne (37). Koshland et al. (37) describe a qualitative model for how depolymerization could drive kinetochore movement, and Hill and Kirschner (5) have shown that such movements are thermodynamically feasible. The BR model fills in the mechanical mechanism, and Eq. 5 may apply to this phenomenon as well.

DISCUSSION

The notion that biased Brownian motion drives certain biological motions is not new: Huxley implied as much in his 1957 model for myosin (38), and later authors have proposed similar models for other molecular motors (1–4, 39). The model we present here differs from these in two respects. Physically, we are modeling mechanisms that do not operate in the same thermodynamic cycle as do molecular motors. Rather they are "one-shot" engines; for example, after protrusion of a filopod the polymers must be disassembled and the process started anew. Mathematically, we do not treat the motion as a biased random walk, as in Feynman's "thermal ratchet" machine (40). Biased random walk models assume asymmetric jump probabilities in either direction at each step; in the limit of small step sizes this produces a continuous drift velocity proportional to the difference in jump

probabilities (41). By contrast, we assume that the jump probabilities are symmetric, and so diffusion is unbiased. Only when diffusion crosses a ratchet threshold does the motion become ratcheted.

Perhaps these differences do not distinguish between thermal mechanisms in any fundamental way, for thermal fluctuations participate in all chemical reactions and, ultimately, the BR mechanism derives its free energy from chemical reactions: actin polymerization in the case of *Listeria* and filopodial motion, and by a variety of processes in protein translocation, including binding of chaperonins, post-translational coiling, glycosylation, etc. As in Huxley's model and its relatives, the proximal *force* for movement arises from random thermal fluctuations, while the chemical potential release accompanying reactions serves to rectify the thermal motions of the load (e.g., Refs. 2 and 42). For example, the binding free energy of a monomer to the end of an actin filament must be tight enough to prevent the load from back diffusion. If ΔG_b were $\sim k_B T$, the residence time of the monomer would be short and the site would likely be empty when the load experiences a reverse fluctuation, or, if the site is occupied, the force of its collision with the load would dislodge the monomer. Hence the concentration of monomers and the binding energy of polymerization supply the free energy to implement the ratchet. Thus these processes do not violate the Second Law; rather they use chemical bond energy to bias the available thermal fluctuations to drive the ratchet.

APPENDICES

A. The polymerization ratchet

In this appendix we derive the load-velocity relation for the polymerization ratchet. Consider the situation shown in Fig. 3.
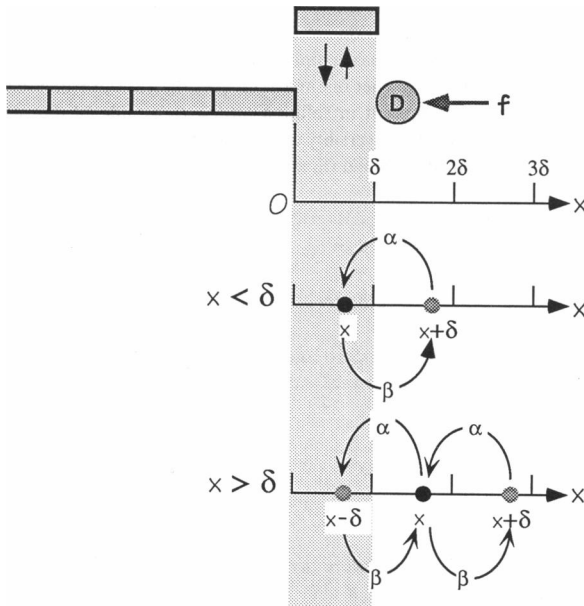

FIGURE 3   Transition diagram for Eqs. A1 and A2.

A particle diffuses in one dimension ahead of a growing polymer. We put the origin of our coordinate system on the tip of the polymer so that the distance between the tip and the diffusing particle is x. The particle executes a continuous random walk (Brownian motion) with diffusion coefficient D in a constant force field, $-f$, which imparts a drift velocity $-Df/k_B T$. Whenever the distance between the particle and the tip of the polymer exceeds the size of a monomer, δ, there is a probability/unit time $\alpha = k_{on} \times$ (monomer concentration) that a monomer will polymerize onto the tip, extending the length of the polymer by δ. This is equivalent to the particle jumping from $x \rightarrow x - \delta$, since x is the distance between the particle and the tip of the polymer. Regardless of the position of the diffusing particle, there is a probability/unit time $\beta = k_{off}$ of a monomer dissociating from the tip of the polymer. This is equivalent to the particle jumping from $x \rightarrow x + \delta$. We describe the mean behavior of a large ensemble of such particle-polymer systems by defining a density $c(x, t)$, such that $\int_a^b c(x, t)\, dx$ = number of systems in the ensemble for which x is in the interval (a, b) at time t. Consulting the transition diagram in Fig. 3, one can see that $c(x, t)$ obeys the following pair of diffusion equations:

$$\frac{\partial c}{\partial t} = D\frac{\partial^2 c}{\partial x^2} + \frac{Df}{k_B T}\frac{\partial c}{\partial x} + \alpha c(x + \delta, t) - \beta c(x, t), \quad x < \delta \quad \text{(A1)}$$

$$\frac{\partial c}{\partial t} = D\frac{\partial^2 c}{\partial x^2} + \frac{Df}{k_B T}\frac{\partial c}{\partial x} + \alpha[c(x + \delta, t) - c(x, t)]$$
$$+ \beta[c(x - \delta, t) - c(x, t)], \quad x > \delta \quad \text{(A2)}$$

With the help of the Heaviside step function, these may be written as a single equation, as has been done in the text (Eq. 1). We will assume that the free energy of polymerization is sufficiently large that a monomer cannot be knocked off if the load fluctuates to the left and hits the tip. Thus we can impose the reflecting boundary condition at $x = 0$ as follows.

$$-D\frac{\partial c(0, t)}{\partial x} - \frac{Df}{k_B T}c(0, t) = 0 \quad \text{(A3)}$$

We also impose the condition that $c(x, t)$ be continuous at $x = \delta$ (this turns out to ensure that the flux is continuous at $x = \delta$ as well):

$$c(\delta_-, t) = c(\delta_+, t). \quad \text{(A4)}$$

Once a steady state solution $c(x)$ has been found for a given load force f, the velocity corresponding to that load is found as follows.

$$v = \delta\frac{\alpha\int_\delta^\infty c(x)\, dx - \beta\int_0^\infty c(x)\, dx}{\int_0^\infty c(x)\, dx} \quad \text{(A5)}$$

This is because $\int_0^\infty c(x)\, dx$ is the total number of systems in the ensemble and $\int_\delta^\infty c(x)\, dx$ is the number of systems for which the gap between the diffusing particle and the polymer tip is large enough for monomer insertion. Thus $\alpha\int_\delta^\infty c(x)\, dx - \beta\int_0^\infty c(x)\, dx$ is the net rate of polymerization (number of monomers inserted minus the number of monomers removed/unit time) for the ensemble as a whole. Dividing by the number of systems in the ensemble, we obtain the net rate of polymerization/system (i.e., per polymer chain). Finally, we multiply by the monomer size, δ, to convert this rate to the velocity with which the polymer tip advances. As a result of this entire computation, we obtain the formula for the mean polymerization velocity as a function of the load force f, as given in the text (Eq. 2).

B. The translocation ratchet

The situation for the translocation ratchet is somewhat different from that of the polymerization ratchet and requires a separate analysis. Consider a rod diffusing longitudinally along the x axis with diffusion coefficient D. A force, $-f$, is applied to the end of the rod which imparts a drift velocity $-(f/\zeta) = -(D/k_B T)f$, where ζ is the frictional drag coefficient. The rod carries ratchet sites which are equally spaced and have separation δ between adjacent sites. We assume that a ratchet site can freely cross the origin from left to right. In the case of a perfect ratchet, we assume that each ratchet site,

and hence the entire rod, is reflected every time a ratchet site attempts to cross the origin from right to left. In the case of an imperfect ratchet, such reflection is not certain, but is assigned a probability, p. In either case, analysis of the situation is facilitated by introducing a variable $X(t)$ = position of the first site to the right of the origin, so that $X(t)$ is always in $(0,\delta)$. Then $X(t)$ describes a (continuous) random walk on a circular domain with a rectifying (or partially rectifying) condition at the origin (see Fig. 4).

The perfect translocation ratchet

Consider an ensemble of such rods, and let $c(x, t)$ be the density of the variable $X(t)$, defined above, so that $\int_a^b c(x, t)$ = number of rods in the interval: $a < X(t) < b$. Then the flux of rods at a point x is as follows.

$$\phi = -\frac{Df}{k_B T} c - D \frac{\partial c}{\partial x}. \tag{B1}$$

The density and flux satisfy the following conservation equation.

$$\frac{\partial c}{\partial t} + \frac{\partial \phi}{\partial x} = 0 \tag{B2}$$

The boundary conditions for this system are as follows.

$$\phi(0, t) = \phi(\delta, t) \tag{B3}$$

$$c(\delta, t) = 0 \tag{B4}$$

The first condition expresses the fact that a new ratchet appears at $x = 0$ each time an old one disappears at $x = \delta$. The second condition expresses the fact that $x = \delta$ is an absorbing boundary, since the ratchet is perfect.

We shall consider only steady states, in which c and ϕ are independent of time. Then, since $\partial c/\partial t = 0$, we also have $\partial \phi/\partial x = 0$, and so ϕ is an unknown constant. The concentration, $c(x,t)$ is obtained by solving Eq. B1
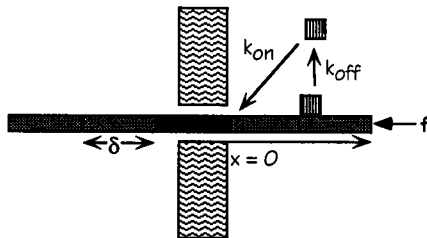
(a)
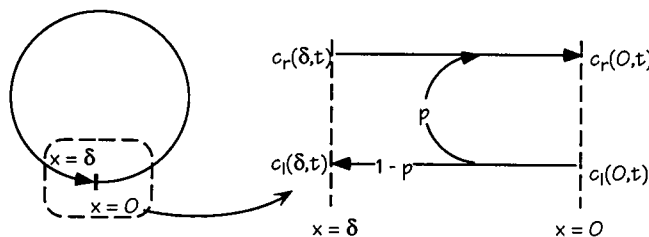
(b)

FIGURE 4   (a) Geometry of the translocation ratchet. Binding sites for chaperonins are spaced δ apart. k_{on} and k_{off} are the binding and dissociation rate constants, respectively. (b) Transition diagram for deriving the boundary condition (B27).

with the boundary condition (Eq. B4). The solution is:

$$c(x) = \frac{k_B T \phi}{Df} \left[e^{\frac{f(\delta - x)}{k_B T}} - 1 \right]. \tag{B5}$$

The number of rods in the ensemble can expressed in terms of the flux, ϕ:

$$N = \int_0^\delta c(x) \, dx = \frac{\phi \delta^2}{D} \left(\frac{k_B T}{f \delta} \right) \left[\exp\left(\frac{f \delta}{k_B T} \right) - 1 - \frac{f \delta}{k_B T} \right]. \tag{B6}$$

The flux ϕ is the average rate at which ratchet sites cross the origin (from left to right) in the ensemble as a whole. Thus ϕ/N is the corresponding rate for an individual rod. Since the rod moves a distance δ for each site ratcheted, the mean velocity of the rod is $\delta \times \phi/N$. Thus we may compute the average velocity of the perfect translocation ratchet as

$$v = \left(\frac{2D}{\delta} \right) \frac{\omega^2/2}{(e^\omega - 1) - \omega} \tag{B7}$$

where $\omega \equiv (f\delta/k_B T)$. At zero load this reduces to the ideal ratchet velocity $v = (2D/\delta)$. Note that as a consequence of assuming that the ratchet is perfect there is no force that will bring the ratchet to a halt. To circumvent this feature we generalize the model as follows.

The imperfect translocation ratchet

Suppose that each site which is located on $x > 0$ can exist in two states that are in rapid equilibrium:

$$S_0 \underset{k_{on}}{\overset{k_{off}}{\rightleftharpoons}} S_1 \tag{B8}$$

and that only sites in the state S_1 are ratcheted. Thus sites in state S_0 pass freely through the origin in both directions, but sites in state S_1 are reflected. Let p be the probability of finding a ratchet in state S_1:

$$p = \frac{k_{on}}{k_{on} + k_{off}} \tag{B9}$$

where k_{on} and k_{off} are the rate constants for the transitions between the two states. The results of this section are valid in the limit $k_{on} \to \infty$, $k_{off} \to \infty$, but in such a way that p has a finite limit. As a physical example of an imperfect Brownian ratchet one may consider the case in which chaperonin molecules are present in solution on the trans side of the membrane ($x > 0$) and can bind reversibly to specific sites on a protein molecule. Such a site is assumed ratcheted (State S_1) when a chaperonin molecule is bound.

In an imperfect ratchet, Eqs. B1, B2, and B3 still apply, but the boundary condition (Eq. B4) is replaced by

$$c(\delta) = (1 - p)c(0). \tag{B10}$$

The justification for this boundary condition is given below. Proceeding as before, we solve for $c(x)$, then N, and compute the velocity as follows.

$$v = \frac{2D}{\delta} \left[\frac{\frac{1}{2}\omega^2}{\left(\frac{(e^\omega - 1)}{1 - K(e^\omega - 1)} \right) - \omega} \right] \tag{B11}$$

Here $\omega = (f\delta/k_B T)$ is the work done against the load force f when the ratchet moves one unit, δ, and $K = (1 - p)/p = k_{off}/k_{on}$ is the dissociation constant of the ratchet. The shape of the load-velocity curve is concave,

decreasing from a no-load velocity of $v_{max} = (2D/\delta)(1/1 + 2K)$ to a stall velocity at $f_0 = (k_B T/\delta) \ln(1 + (1/K))$. For the ranges of parameters we shall employ, the force-velocity curve is practically linear and can be approximated by

$$v \approx v_{max} \left(1 - \frac{f}{f_0}\right) = \frac{2D}{\delta} \frac{1}{1 + 2K} \left(1 - \frac{f\delta/k_B T}{\ln((K + 1)/K)}\right). \qquad (B12)$$

Deriviation of the boundary condition

The boundary condition $c(\delta) = (1 - p)c(0)$ is crucial to the derivation of the ratchet equation. To see where it comes from we proceed as follows. The diffusion equation implies an infinite speed for a Brownian particle and equal probabilities of stepping to the right or left (41). Therefore, we examine the limit of a finite speed random walk by defining density functions for points moving to the right, $c_r(x,t)$, and to the left, $c_l(x, t)$. with speed s. These obey the conservation equations:

$$\frac{\partial c_r}{\partial t} + s\frac{\partial c_r}{\partial x} = -\gamma_{lr}c_r + \gamma_{rl}c_l \qquad (B13)$$

$$\frac{\partial c_l}{\partial t} - s\frac{\partial c_l}{\partial x} = \gamma_{lr}c_r - \gamma_{rl}c_l \qquad (B14)$$

Here γ_{rl} and γ_{lr} are the probabilities per unit time of a point changing direction from left to right and right to left, respectively. We shall solve these equations on the circular domain $(0, \delta)$ using the following transition rules at the origin $x = 0 = \delta$ (cf. Fig. 4). Points moving to the right cross the origin and continue to the right. Leftward moving points encountering the boundary have a probability p of reversing their direction and a probability $(1 - p)$ of maintaining their direction. This translates into the following conditions on the fluxes of particles at the origin as follows.

$$sc_r(\delta, t) + sp \times c_l(0, t) = sc_r(0, t) \qquad (B15)$$

$$sc_l(\delta, t) = s(1 - p) \times c_l(0, t) \qquad (B16)$$

Dividing by s and rearranging yields:

$$c_r(\delta, t) = c_r(0, t) - pc_l(0, t) \qquad (B17)$$

$$c_l(\delta, t) = (1 - p) \times c_l(0, t). \qquad (B18)$$

Rather than solving for c_r and c_l, we shall solve for their sum and difference:

$$c(x, t) = c_r(x, t) + c_l(x, t) \qquad (B19)$$

$$u(x, t) = c_r(x, t) - c_l(x, t). \qquad (B20)$$

Adding and subtracting the conservation equations yields:

$$\frac{\partial c}{\partial t} + s\frac{\partial u}{\partial x} = 0 \qquad (B21)$$

$$\frac{\partial u}{\partial t} + s\frac{\partial c}{\partial x} = \nu c - \gamma u \qquad (B22)$$

where $\nu = \gamma_{rl} - \gamma_{lr}$, and $\gamma = \gamma_{rl} + \gamma_{lr}$. We can reduce this to a single equation in $c(x_2 t)$ by eliminating the unknown u and defining $S^2/\gamma \equiv D$ and $\nu/s \equiv -f/k_B T$ as follows.

$$\frac{1}{\gamma}\frac{\partial^2 c}{\partial t^2} + \frac{\partial c}{\partial t} - \frac{Df}{k_B T}\frac{\partial c}{\partial x} = D\frac{\partial^2 c}{\partial x^2} \qquad (B23)$$

As $s \to \infty$ with D and f fixed, this becomes

$$\frac{\partial c}{\partial t} = D\frac{\partial^2 c}{\partial x^2} + \frac{Df}{k_B T}\frac{\partial c}{\partial x} \qquad (B24)$$

which is equivalent to Eqs. B1–B2. The boundary condition for this equation may be deduced from Eqs. B17 and B18; it is as follows.

$$c(\delta, t) = c(0, t) - p2c_l(0, t) = (1 - p) \times c(0, t) + p \times u(0, t). \qquad (B25)$$

This boundary condition contains the variable u, which we now show vanishes in the limit considered above. Dividing the equation for $\partial u/\partial t$ by γ:

$$\frac{1}{\gamma}\frac{\partial u}{\partial t} + \frac{s}{\gamma}\frac{\partial c}{\partial x} = \left(\frac{\nu}{\gamma}\right) c - u. \qquad (B26)$$

Now, let $\gamma \to \infty$ (with D and f fixed), and note that $s/\gamma = \sqrt{D\gamma}/\gamma \to 0$, $\nu/\gamma = (-Df/k_B T)(1/s) = (-Df/k_B T) \times (1 \times \sqrt{D\gamma}) \to 0$ (with D and f fixed). Therefore, $u \to 0$ as $\gamma \to \infty$; that is, as the reversal rate, γ gets very large, the random walk becomes symmetric (41). Since $u \to 0$, the limiting form of the boundary condition on c is as follows.

$$c(\delta, t) = (1 - p) \times c(0, t) \qquad (B27)$$

C. *Listeria* velocity is proportional to tail length

Using fluorescently tagged actin monomers Theriot and Mitchison (21) demonstrated that the velocity of a bacterium varies linearly with the length of its actin tail. We can describe these experiments as follows. In the lab frame, the tail is stationary and the bacterium moves (say, to the right) at velocity $v > 0$. In a coordinate system attached to the bacterium, the tail has velocity $-v$, and the posterior edge of the bacterium is located at some fixed position, say $x = 0$. Let $n(x, t)$ be the density of short actin filaments in the tail at position x and time t. Then the conservation equation for the fiber density is:

$$\frac{\partial n}{\partial n} - \frac{\partial}{\partial x}(n \times v) = -\mu n \qquad (C1)$$

where v is the bacterial velocity so that $-v$ is the velocity of the tail relative to the bacterium, and μ is the local rate of actin depolymerization; Eq. C1 holds on $x < 0$. Let us consider the steady state situation, $(\partial n/\partial t) = 0$. The boundary condition for this equation is simply that the flux of tail material at the bacterial interface is equal to the polymerization rate:

$$v \times n(0) = \psi \equiv \text{polymerization rate.} \qquad (C2)$$

At steady state ψ is constant and the solution to the conservation equation is

$$n(x) = n(0)\exp\left(\frac{\mu x}{v}\right) = \frac{\Psi}{v}\exp\left(\frac{\mu x}{v}\right), \quad x < 0. \qquad (C3)$$

Note that the space constant for the exponential decay of the tail density is $L = v/\mu$; in this sense, the length of the tail is proportional to v. Therefore, the length of the tail will be proportional to v, and the slope of the L vs. v curve simply measures the rate of depolymerization of the tail meshwork. Thus the linearity of velocity with tail length does not tell us anything about the mechanism of locomotion.

REFERENCES

1. Mitsui, T., and H. Ohshima. 1988. A self-induced model of myosin head motion in contracting muscle. I. Force-velocity relation and energy liberation. *J. Muscle Res. Cell Motil.* 9:248–260.

2. Meister, M., S. R. Caplan, and H. C. Berg. 1989. Dynamics of a tightly coupled mechanism for flagellar rotation: bacterial motility, chemiosmotic coupling, protonmotive force. *Biophys. J.* 55:905–914.

3. Cordova, N., B. Ermentrout, and G. Oster. 1991. The mechanics of motor molecules. I. The thermal ratchet model. *Proc. Natl. Acad. Sci. USA.* 89:339–343.

4. Vale, R. D., and F. Oosawa. 1990. Protein motors and Maxwell's demons: does mechanochemical transduction involve a thermal ratchet? *Adv. Biophys.* 26:97–134.

5. Hill, T., and M. Kirschner. 1982. Bioenergetics and kinetics of microtubule and actin filament assembly and disassembly. *Int. Rev. Cytol.* 78:1–125.

6. Janmey, P., C. Cunningham, G. Oster, and T. Stossel. 1992. Cytoskeletal networks and osmotic pressure in relation to cell structure and motility. *In* Swelling Mechanics: From Clays to Living Cells and Tissues. T. Karalis, editor. Springer-Verlag, Heidelberg.

7. Miyamoto, H., and H. Hotani. 1988. Polymerization of microtubules within liposomes produces morphological change of their shapes. *In* Taniguchi International Symposium on Dynamics of Microtubules. H. Hotani, editor. The Taniguchi Foundation, Taniguchi, Japan. 220–242.

8. Bo, L., and R. E. Waugh. 1989. Determination of bilayer membrane bending stiffness by tether formation from giant, thin-walled vesicles. *Biophys. J.* 55:509–517.

9. Duwe, H., J. Kaes, and E. Sackmann. 1990. Bending elastic moduli of lipid bilayers-modulation by solutes. *J. Phys. II (France).* 51:945–962.

10. Gordon, D., Y.-Z. Yang, and E. Korn. 1976. Polymerization of Acanthamoeba actin. *J. Biol. Chem.* 251:7474–7479.

11. Hill, T., and M. Kirschner. 1983. Regulation of microtubule and actin filament assembly-disassembly by associated small and large molecules. *Int. Rev. Cytol.* 84:185–234.

12. Pollard, T. 1986. Rate constants for the reactions of ATP- and ADP-actin with the ends of actin filaments. *J. Cell Biol.* 103:2747–2754.

13. Argiro, V., M. Bunge, and M. Johnson. 1985. A quantitative study of growth cone filopodial extension. *J. Neurosci. Res.* 13:149–162.

14. Perelson, A. S., and E. A. Coutsias. 1986. A moving boundary model of acrosomal elongation. *J. Math. Biol.* 23:361–379.

15. Oster, G., and A. Perelson. 1988. The physics of cell motility. *In* Cell Behavior: Shape, Adhesion and Motility. J. Heaysman, C. Middleton. F. Watt, editors. 35–54.

16. Oster, G., A. Perelson, and L. Tilney. 1982. A mechanical model for acrosomal extension in *Thyone. J. Math. Biol.* 15:259–265.

17. Tilney, L., and S. Inoué. 1982. The acrosomal reaction of *Thyone* sperm. II. The kinetics and possible mechanism of acrosomal process elongation. *J. Cell Biol.* 93:820–827.

18. Inoué, S., and L. Tilney. 1982. The acrosomal reaction of *Thyone* sperm. II. Changes in the sperm head visualized by high resolution video microscopy. *J. Cell Biol.* 93:812–820.

19. Tilney, L., and S. Inoue. 1985. Acrosomal reaction of the *Thyone* sperm. III. The relationship between actin assembly and water influx during the extension of the acrosomal process. *J. Cell Biol.* 100:1273–1283.

20. Bray, D., N. Money, F. Harold, and J. Bamburg. 1991. Responses of growth cones to changes in osmolality of the surrounding medium. *J. Cell Sci.* 98:507–515.

21. Theriot, J. A., T. J. Mitchison, L. G. Tilney, and D. A. Portnoy. 1992. The rate of actin-based motility of intracellular *Listeria monocytogenes* equals the rate of actin polymerization. *Nature (Lond.).* 357:257–260.

22. Tilney, L. G., and D. A. Portnoy. 1989. Actin filaments and the growth, movement, and spread of the intracellular bacterial parasite, *Listeria monocytogenes. J. Cell Biol.* 109:1597–1608.

23. Dabiri, G. A., J. M. Sanger, D. A. Portnoy, and F. S. Southwick. 1990. *Listeria monocytogenes* moves rapidly through the host-cell cytoplasm by inducing directional actin assembly. *Proc. Natl. Acad. Sci. USA.* 87:6068–6072.

24. Sanger, J. M., J. W. Sanger, and F. S. Southwick. 1992. Host cell actin assembly is necessary and likely to provide the propulsive force for intracellular movement of *Listeria monocytogenes. Infect. Immun.* 60:3609–3619.

25. Berg, H. 1983. Random Walks in Biology. Princeton University Press. Princeton, New Jersey.

26. Pollard, T. 1990. Actin. *Curr. Opin. Cell Biol.* 2:33–40.

27. Cooper, J. A. 1991. The role of actin polymerization in cell motility. *Ann. Rev. Physiol.* 53:585–605.

28. Forscher, P., C. H. Lin, and C. Thompson. 1992. Indictopodia: a novel form of stimulus-evoked growth cone motility involving site directed actin filament assembly. *Nature (Lond.).* 357:515–518.

29. Simon, S., C. Peskin, and G. Oster. 1992. What drives the translocation of proteins? *Proc. Natl. Acad. Sci. USA.* 89:3770–3774.

30. Simon, S., and B. Blobel. 1991. A protein-conducting channel in the endoplasmic reticulum. *Cell.* 65:371–380.

31. de Gennes, P. 1983. Reptation d'une chaine heterogene. *J. Physique Lett.* 44:L225-L227.

32. Cheng, M. Y., F. U. Hartl, J. Martin, R. A. Pollock, F. Kalousek, W. Neupert, E. M. Hallberg, R. L. Hallberg, and A. L. Horwich. 1989. Mitochondrial heat-shock protein hsp60 is assential for assembly of proteins imported into yeast mitochondria. *Nature (Lond.).* 337:620–625.

33. Ostermann, J., A. L. Horwich, W. Neupert, and F. U. Hartl. 1989. Protein folding in mitochondria requires complex formation with hsp60 and ATP hydrolysis. *Nature (Lond.).* 341:125–130.

34. Kagan, B., A. Finkelstein, and M. Colombini. 1981. Diptheria toxin fragment forms large pores in phospholipid bilayer membranes. *Proc. Natl. Acad. Sci. USA.* 78:4950–4954.

35. Ooi, C., and W. J. Weiss. 1992. Bidirectional movement of a nascent polypeptide across microsomal membranes reveals requirements for vectorial translocation of proteins. *Cell.* 71:87–96.

36. Liu, S.-C., L. Derick, S. Zhai, and J. Palek. 1991. Uncoupling of the spectrin-based skeleton from the lipid bilayer in sickled red cells. *Science.* 252:574–575.

37. Koshland, D. E., T. J. Mitchison, and M. W. Kirschner. 1988. Polewards chromosome movement driven by microtubule depolymerization in vitro. *Nature (Lond.).* 331:499–504.

38. Huxley, A. F. 1957. Muscle structure and theories of contraction. *Prog. Biophys. Biophys. Chem.* 7:255–318.

39. Leibler, S., and D. Huse. 1991. A physical model for motor proteins. *C. R. Acad. Sci. (III).* 313:27–35.

40. Feynman, R., R. Leighton, and M. Sands. 1963. The Feynman Lectures on Physics. Addison-Wesley, Reading, MA.

41. Zauderer, E. 1989. First order partial differential equations. *In* Partial Differential Equations of Applied Mathematics. John Wiley & Sons, New York.

42. Khan, S., and H. C. Berg. 1983. Isotope and thermal effects in chemiosmotic coupling to the flagellar motor of *Streptococcus. Cell.* 32:913–919.